ISSN No:-2456-2165 https://doi.org/10.38124/ijisrt/26aug1216

Uranium Polishing from African Copperbelt Cobalt Process Liquors Using Phosphoric Acid

Mechanisms, Thermodynamic Constraints, Process Evidence, and Research Requirements

Roger K. M. Rumbu[1]

[1]MSc Metallurgy and Materials Science Polytechnics Faculty, University of Kolwezi, D.R. Congo

Publication Date: 2026/09/10

Abstract: Phosphoric-acid treatment is used to remove uranium from selected African Copperbelt cobalt process liquors. This structured critical review develops a comparative decision framework linking uranium-retention mechanisms, phosphorus demand, and cobalt-product acceptance. Industrial accounts, laboratory experiments, dissolution studies, and conceptual process comparisons are appraised separately. The synthesis distinguishes discrete uranyl-phosphate precipitation, adsorption, and incorporation into host solids. It shows why a decrease in filtered uranium does not establish a unique retention mechanism or cobalt selectivity. Calcium-bearing hosts, reagent-derived metals, colloid capture, and uranium already present in seeds change the interpretation of dose and removal. A phosphorus-to-uranium molar ratio of one corresponds conditionally to 0.4117 kg pure H_3PO_4 per kilogram uranium. Sampling-inclusive balances connect this stoichiometric basis to measured transfer, while a downstream balance includes uranium retained in solids, entrained liquor, cobalt yield, and dry or wet product mass. Bicarbonate dissolution evidence makes residue acceptance dependent on exposure chemistry and duration. Economic reconciliation distinguishes reported payback conventions from unresolved reagent-consumption assumptions. The contribution is an evidence-to-decision framework: identify the phosphorus sinks, close uranium and cobalt inventories, discriminate the uranium host, and verify separation and product quality before selecting a site-specific dose.

Keywords: *African Copperbelt, Cobalt Liquor, Phosphoric Acid, Uranium, Phosphate Precipitation, Ion Exchange, Mass Balance.*

How to Cite: Roger K. M. Rumbu (2026) Uranium Polishing from African Copperbelt Cobalt Process Liquors Using Phosphoric Acid. *International Journal of Innovative Science and Research Technology*, 11(8), 3261-3278. https://doi.org/10.38124/ijisrt/26aug1216

I. INTRODUCTION

African Copperbelt cobalt recovery commonly follows sulfuric-acid leaching, copper SX, and staged impurity removal. Uranium associated with selected ore domains introduces an additional separation requirement. A low dissolved uranium concentration before cobalt precipitation is desirable, but its relationship to final-product quality depends on uranium deportment, cobalt precipitation yield, cake moisture, washing, and the applicable product specification. The regional flowsheet context is described by Sole et al. (2019) and Crundwell et al. (2020). Manzuk and Philippe (2026) address uranium in cobalt-hydroxide exports and reinforce the relevance of uranium accounting.

This review asks which observations support phosphoric-acid uranium polishing and which measurements are needed to convert those observations into a defensible process decision. Its original contribution is the comparative framework, rather than a new equilibrium constant or treatment experiment. The framework connects three retention mechanisms to their competing explanations and discriminating measurements, then links the resulting U–Co–P inventories to dose and cobalt-product acceptance. It yields four decision rules: identify the phosphorus sinks before assigning dose, interpret filtered depletion through a complete inventory, establish the uranium host with complementary evidence, and verify separation and product quality under the intended operating and residue-exposure conditions.

The scientific synthesis proceeds from aqueous chemistry and accounting to source comparison and process interpretation. Section 7 consolidates the limits of the evidence. Section 8 translates the framework into an experimental programme, and Section 9 connects the results to treatment placement and operational decisions.

ISSN No:-2456-2165 https://doi.org/10.38124/ijisrt/26aug1216

II. REVIEW METHOD

➢ *Scope, Retrieval, and Selection*

This structured critical review emphasizes publications from 2006 onward concerning uranium in cobalt-processing streams, uranium-phosphate chemistry, phase-specific thermodynamics, and the measurement of treatment performance. Sources were retained for direct relevance to cobalt hydrometallurgy or for resolving a specific mechanistic question concerning phosphate precipitation, adsorption, incorporation, or dissolution. Studies of environmental matrices provide mechanistic evidence and remain separate from industrial performance evidence.

Literature retrieval on 5 September 2026 used a public web-search interface for subject, exact-title, author, and DOI queries, followed by publisher and institutional records and the 2RA-Edition Archive search interface. The underlying web-search index was not disclosed. Complete queries, coverage restrictions, and study dispositions are recorded in Supplement S1. English-language publications from 2006 through the search date were eligible. Full papers were available for Mehta et al. (2014), Lammers et al. (2017), Foster et al. (2019), Szenknect et al. (2020), and Rao et al. (2026). The Gudavalli et al. (2013) paper was obtained through 2RA-Edition. Catalogue records served as discovery aids. Quantitative claims were checked against the source papers. The search was targeted, and no exhaustive database coverage or reconstructed screening count is claimed.

Full-text extraction covers twelve central studies. Mehta et al. (2016) is retained only for the qualitative pathway findings disclosed in its abstract, with inaccessible methods fields identified in Supplement S1. Exact concentration plateaus are not reconstructed for Gorman-Lewis et al. (2009), whose main paper was inspected but supporting concentration tables were inaccessible. These access restrictions determine which claims enter the synthesis.

Duplicate DOI records were treated as one study. The thirteen central studies were retained for operational relevance, analytical feasibility, process comparison, pathway discrimination, equilibrium assessment, or residue release. Their individual selection decisions and the four-question appraisal appear in Supplement S1. Other cited sources support chemical conventions and process context. Environmental studies are retained for mechanism, with industrial transfer assessed separately. Wet-process phosphoric-acid uranium recovery is outside the cobalt-liquor treatment question. Search results without an inspectable study basis were excluded from quantitative inference. No removal percentages from incompatible matrices were pooled.

➢ *Evidence Classification and Extraction*

Table 1 defines the evidence categories. These categories describe the kind of evidence, not an automatic ranking of scientific quality. An operational account with limited measurement disclosure has high process relevance but low quantitative reproducibility. A well-characterized laboratory system has greater mechanistic resolution but limited industrial transferability.

Table 1 Evidence Classes and Permissible Inference.

Class	Evidence type	Permissible inference
A	Reported cobalt-plant operation or actual cobalt-liquor tests	Site-specific experience, subject to disclosed measurements
B	Laboratory experiment or environmental field test	Mechanism or measured performance in the tested matrix
C	Thermodynamic or transport study	Interpretation within the stated reactions and model domain
D	Flowsheet overview or proposed application	Process context or a hypothesis requiring demonstration

Extraction records the source location, tested or assumed matrix, reagent basis, pH, time and temperature where available, uranium response, cobalt measurements, and solid-phase evidence. Numerical values are labelled as measurements, source-reported estimates, or design assumptions. “Not verified” denotes an access-limited field. “Not reported” is reserved for information absent from an inspected full text. Table 3 provides the study index. Supplement S1 provides the uniform extraction matrix, exact source locations, selection record, and study-specific appraisal.

Four questions govern quality appraisal: does the source represent cobalt liquor, are the relevant conditions disclosed, are uranium removal and cobalt retention jointly measured, and is the uranium-bearing phase identified? Claims of a universal dose or operating range require broader support than any single category supplies. Heterogeneous matrices and incomplete uncertainty reporting prevent defensible statistical pooling in this review.

III. URANIUM TRANSFER AND PROCESS PLACEMENT

Dissolved U(VI) forms sulfate complexes during acidic processing. The following balanced stepwise relations identify possible species (Vercouter et al., 2008, Vopálka et al., 2010):

$$UO_2^{2+} + SO_4^{2-} \rightleftharpoons UO_2SO_4^0 \quad (1)$$

$$UO_2SO_4^0 + SO_4^{2-} \rightleftharpoons UO_2(SO_4)_2^{2-} \quad (2)$$

$$UO_2(SO_4)_2^{2-} + SO_4^{2-} \rightleftharpoons UO_2(SO_4)_3^{4-} \quad (3)$$

Species fractions depend on free sulfate activity, bisulfate dissociation, pH, temperature, and the equilibrium

ISSN No:-2456-2165 https://doi.org/10.38124/ijisrt/26aug1216

data adopted. Neutral complexes do not contribute directly to anion-exchange loading in the same manner as anionic species. Anionic uranyl complexes provide a chemical basis for separation from cationic cobalt, but resin performance also depends on competing anions, mass transfer, fouling, elution, and equipment operation. Avelar et al. (2017) illustrate the importance of sulfate-complexation assumptions in uranium solvent-extraction modelling.

Treatment placement follows the process relationships described by Sole et al. (2019) and Crundwell et al. (2020). Phosphate dosing location requires coordination with residual copper and FAM removal, available neutralization capacity, and separation of newly formed solids. Combining removal stages changes which precipitates consume phosphorus and which solids carry cobalt.

➢ *Phosphoric-Acid Polishing Chemistry and Accounting*

- *Free Phosphate, Total Phosphorus, and Candidate Solids*

The acid-dissociation reactions are:

$$H_3PO_4 \rightleftharpoons H^+ + H_2PO_4^- \quad (4)$$

$$H_2PO_4^- \rightleftharpoons H^+ + HPO_4^{2-} \quad (5)$$

$$HPO_4^{2-} \rightleftharpoons H^+ + PO_4^{3-} \quad (6)$$

At 25 °C, conventional dilute-aqueous reference values are approximately 2.15, 7.20, and 12.35 for the three pK_a values (Haynes et al., 2016). They are not conditional plant constants. For an ideal solution, write $H = a_{H^+}$ and:

$$D = H^3 + K_{a1}H^2 + K_{a1}K_{a2}H + K_{a1}K_{a2}K_{a3} \quad (7)$$

$$\alpha_0 = \frac{H^3}{D}, \quad \alpha_1 = \frac{K_{a1}H^2}{D}, \quad \alpha_2 = \frac{K_{a1}K_{a2}H}{D}, \quad \alpha_3 = \frac{K_{a1}K_{a2}K_{a3}}{D} \quad (8)$$

These fractions refer only to the uncomplexed pool consisting of H_3PO_4, $H_2PO_4^-$, HPO_4^{2-}, and PO_4^{3-}. Define its molality as $b_{P,free}$. Total dissolved phosphorus, $b_{P,T}$, additionally includes phosphorus in metal complexes. In a non-ideal liquor, concentrations or molalities cannot be obtained by inserting hydrogen activity into Equation (8) while ignoring the different activity coefficients of the phosphate species. Annex A gives the corresponding mass-action ratios and total-phosphorus expression.

For illustration of the stated ideal formula, pH 4 gives approximately 98.55% $H_2PO_4^-$, 1.39% H_3PO_4, and 0.062% HPO_4^{2-} within the free pool. These calculated fractions are not plant measurements or a recommended pH. Low free PO_4^{3-} does not preclude precipitation because acid dissociation and complex dissociation replenish consumed species.

Candidate uranyl-phosphate complexes include:

$$UO_2^{2+} + HPO_4^{2-} \rightleftharpoons UO_2HPO_4^0 \quad (9)$$

$$UO_2^{2+} + PO_4^{3-} \rightleftharpoons UO_2PO_4^- \quad (10)$$

A calcium-bearing phosphate sink is represented by:

$$2UO_2^{2+} + Ca^{2+} + 2HPO_4^{2-} + nH_2O \rightleftharpoons Ca(UO_2)_2(PO_4)_2 \cdot nH_2O(s) + 2H^+ (11)$$

Equation (11) conserves atoms and charge and shows proton release. It identifies a candidate stoichiometry, not an industrial mineral determination. Hydronium uranyl phosphate, uranyl orthophosphate, and calcium uranyl phosphates require separate phase definitions and equilibrium constants (Gorman-Lewis et al., 2009). Hydrate state is consequential: autunite and meta-autunite are not interchangeable names for thermodynamic calculations. Dzik et al. (2017) examine synthetic autunite thermodynamics and dehydration-related stability.

Adsorption and incorporation into another precipitate require different evidence from formation of a separate crystalline uranium phosphate. XRD identifies sufficiently abundant crystalline material. SEM-EDS provides elemental association rather than a unique crystal structure. Poorly crystalline or trace uranium hosts require complementary spectroscopy and chemical balances.

- *Sulfate, Carbonate, and Competing Cations*

Sulfate complexation decreases free uranyl activity relative to total dissolved U(VI). Carbonate and calcium introduce additional complexes (Dong and Brooks, 2006):

$$UO_2^{2+} + 3CO_3^{2-} \rightleftharpoons UO_2(CO_3)_3^{4-} \quad (12)$$

$$UO_2^{2+} + 2Ca^{2+} + 3CO_3^{2-} \rightleftharpoons Ca_2UO_2(CO_3)_3^0 \quad (13)$$

A complete calculation should also consider other supported carbonate species, including the singly calcium-bearing ternary complex. The importance of carbonate is conditional on pH, DIC, calcium, and gas exchange. Its existence does not prove dominance in acidic sulfate liquor. Mehta et al. (2014) show that co-solutes and solution conditions affect phosphate products and residual uranium. Their results motivate measurement of DIC rather than an assumed carbonate concentration.

Residual Fe, Al, Ca, Mg, and Co introduce phosphate consumption or coprecipitation pathways. Calcium has a dual role: it participates in candidate uranium-bearing solids and competes for phosphorus in calcium phosphates. Existing FAM solids provide sorption and nucleation surfaces. Filtered and unfiltered liquor tests therefore address different mechanisms, and their results should not be pooled without identifying the solid inventory.

- *Stoichiometry, Commercial Reagent, and Dose Factor*

Let $m(i)$ be component mass, $\mathcal{M}_i$ molar mass, and $n(i) = m(i)/\mathcal{M}_i$ amount of substance. The stoichiometric molar ratio $r_{P/U,st}$ is fixed by the assumed solid. If added H_3PO_4 supplies all phosphorus incorporated in that solid:

$$R_{acid/U,th} = \frac{m(H_3PO_4)}{m(U)} = r_{P/U,st}\frac{\mathcal{M}_{H_3PO_4}}{\mathcal{M}_U} = 0.4117 r_{P/U,st} \quad (14)$$

ISSN No:-2456-2165 https://doi.org/10.38124/ijisrt/26aug1216

The molar masses 97.994 and 238.029 g mol⁻¹ give a ratio of 0.411689 (Meija et al., 2016). A P/U ratio of one gives 0.4117 kg pure H_3PO_4 kg⁻¹ U. A ratio of two-thirds, appropriate to $(UO_2)_3(PO_4)_2$, gives 0.2745 kg kg⁻¹. These are conditional requirements for the designated phosphate pathway. Existing phosphate, adsorption, and uranium incorporation in other solids change the external acid requirement. Competing sinks and residual dissolved phosphorus increase the demand attributed to added reagent.

Define $r_{\mathrm{P/U,op}} = n(\mathrm{P,added})/n(\mathrm{U,target})$, where the denominator is the uranium removal required on the selected inventory or throughput basis. Actual phosphorus addition is computed from the reagent assay. The operating molar ratio does not contain a second purity correction. Commercial acid mass fraction is applied once when converting moles or pure-acid equivalent into solution mass or volume.

The dose factor is $F_{\mathrm{dose}} = r_{\mathrm{P/U,op}}/r_{\mathrm{P/U,st}}$. For the same phosphorus source and mechanism, $F_{\mathrm{dose}} = 1$ denotes stoichiometric dosing and $100(F_{\mathrm{dose}} - 1)$ is the percentage excess. Values below one should trigger investigation of other phosphorus sources or removal pathways, not an automatic mass-balance rejection. This factor is not a measurement of residual phosphate.

A competing cobalt phase is:

$$3\mathrm{Co}^{2+} + 2\mathrm{PO}_4^{3-} \rightleftharpoons \mathrm{Co}_3(\mathrm{PO}_4)_2(\mathrm{s}) \quad (15)$$

Its saturation state depends on free-ion activities and the specific solid selected. Cobalt entrainment, adsorption, and incorporation in mixed precipitates must also be assessed. Formation of the phase in Equation (15) is not established by cobalt loss alone.

- *Batch Accounting with Sampling Corrections*

For an initially dissolved batch inventory with no added uranium, define the uranium remaining in all accounted aqueous fractions by:

$$m_{\mathrm{U,aq,accounted}} = C_{\mathrm{U},f}V_f + \sum_k C_{\mathrm{U},k}\,\Delta V_k + m_{\mathrm{U,other\ aq}}$$

The final term includes distinct aqueous fractions, such as recovered washes, only when they are not already represented by another term. For samples containing solids, their uranium-bearing solids require separate accounting. The inferred non-aqueous transfer is:

$$\eta_{\mathrm{U,non-aq}} = \left(1 - \frac{m_{\mathrm{U,aq,accounted}}}{C_{\mathrm{U},0}V_0}\right)100\% \quad (16)$$

Equation (16) corrects for dissolved uranium withdrawn during sampling. A change in retained volume alone does not make this correction. The inferred transfer includes precipitation, adsorption, and retained deposits until solid analyses distinguish them. Unmeasured vessel deposits or losses invalidate a mechanistic interpretation. Where reagents add uranium or the feed contains particulate uranium, use the general balance in Annex B instead.

Define the corresponding cobalt inventory consistently:

$$R_{\mathrm{Co,aq}} = \frac{C_{\mathrm{Co},f}V_f + \sum_k C_{\mathrm{Co},k}\,\Delta V_k + m_{\mathrm{Co,other\ aq}}}{C_{\mathrm{Co},0}V_0}100\% \quad (17)$$

$$L_{\mathrm{Co,non-aq}} = 100\% - R_{\mathrm{Co,aq}} \quad (18)$$

This is an accounting measure of aqueous cobalt retention, not final plant recovery. A product-liquor yield should be reported separately when samples and washes are not returned to the process. Use washed-solid cobalt assays, independently measured entrained liquor, and balance closure to interpret the complement in Equation (18).

- *Continuous Balances, Deportment, and Reagent Flow*

For a defined control volume, let I_{P} denote its phosphorus mass inventory:

$$\frac{dI_{\mathrm{P}}}{dt} = \sum_s \dot{m}_{\mathrm{P,in},s} - \sum_s \dot{m}_{\mathrm{P,out},s} \quad (19)$$

Each physical stream appears once. Residual dissolved phosphorus is carried in product liquor, bleed, wash liquor, or another actual stream. It is not an additional outlet to be counted alongside the same product liquor. Account for phosphorus entering in feed and recycle as well as reagent. At steady state the inventory derivative is zero. Dynamic dosing requires the accumulation term.

For a batch with total uranium input $m_{\mathrm{U,in}}$:

$$X_{\mathrm{U,solid}} = \frac{m_{\mathrm{U,solid,accounted}}}{m_{\mathrm{U,in}}}, \quad X_{\mathrm{U,aq}} = \frac{m_{\mathrm{U,aq,accounted}}}{m_{\mathrm{U,in}}} \quad (20)$$

All samples and endpoint fractions belong in the relevant sum. An explicit unaccounted fraction is preferable to forcing the two quantities to sum to one. Define a deportment selectivity ratio using the same accounting boundary:

$$S_{\mathrm{U/Co}} = \frac{m_{\mathrm{U,solid,accounted}}/m_{\mathrm{U,in}}}{m_{\mathrm{Co,solid,accounted}}/m_{\mathrm{Co,in}}} \quad (21)$$

The ratio becomes unstable as measured cobalt transfer approaches zero. Report absolute uranium transfer, cobalt transfer, LOQs, and uncertainty alongside it. If cobalt in the solid is below quantification, report an appropriate bound rather than infinite selectivity.

A validated operating ratio converts to commercial reagent flow as:

$$Q_{\mathrm{acid}} = \frac{\dot{m}_{\mathrm{U,target}}r_{\mathrm{P/U,op}}\mathcal{M}_{\mathrm{H_3PO_4}}}{\mathcal{M}_{\mathrm{U}}w_{\mathrm{acid}}\rho_{\mathrm{acid}}} \quad (22)$$

ISSN No:-2456-2165 https://doi.org/10.38124/ijisrt/26aug1216

Here w_{acid} is assayed H_3PO_4 mass fraction and ρ_{acid} is solution density at the relevant temperature. With uranium flow in kg h^{-1}, density in kg L^{-1}, and consistent molar-mass units, Q_{acid} is L h^{-1}. This relation calculates a flow from an established ratio. It does not establish the ratio, and it becomes unreliable near zero uranium loading if other phosphate sinks remain substantial.

Table 2 Principal Symbols and Reporting Basis.

Symbol	Definition	Unit or convention
a_i	Species activity	Dimensionless, stated standard state
b_i	Species molality	mol kg^{-1} water
C_i	Element mass concentration in balance equations	mg L^{-1} or kg m^{-3}, consistently converted
V, ΔV_k	Liquid inventory, withdrawn sample volume	L or m^3
m_i, $\dot{m}_i$	Element mass, element mass flow	kg, kg h^{-1}
$\mathcal{M}_i$	Molar mass	g mol^{-1} or kg mol^{-1}
I_i	Element inventory within the control volume	kg
$r_{\text{P/U}}$	Molar phosphorus/uranium ratio	mol P mol^{-1} U, stated basis
w_{acid}	Commercial H_3PO_4 mass fraction	kg H_3PO_4 kg^{-1} solution
E_h	Potential relative to SHE	V
SI	Mineral saturation index	Dimensionless

- *From Polished Liquor to Cobalt-Product Quality*

Define a downstream control volume covering cobalt precipitation, filtration, and washing over one batch or a matched steady-state interval. Let $C_{\text{U,p}}$ and V_p describe the polished feed liquor. Include incoming particulate uranium and uranium in reagents, wash water, or additional streams:

$$m_{\text{U,in,Co}} = C_{\text{U,p}} V_p + m_{\text{U,part,in}} + \sum_j m_{\text{U,add},j} \quad (23)$$

Let $f_{\text{U,s}}$ be the fraction of this total uranium input retained in the recovered solid phase after washing, excluding retained pore liquor. Let $C_{\text{U,e}}$ and V_e be the uranium concentration and volume of the liquid retained in the final cake. Then:

$$m_{\text{U,product}} = f_{\text{U,s}} m_{\text{U,in,Co}} + C_{\text{U,e}} V_e \quad (24)$$

The solid term includes uranium precipitated, adsorbed, incorporated, or carried into the recovered solids. The liquid term counts entrainment once. Measure the retained-liquid composition after washing. Substitution of the feed concentration would require evidence of unchanged composition. Filtrate and wash effluents remain separate balance outputs. Determine $f_{\text{U,s}}$ from solid assays and full closure, rather than assuming it equals the polishing removal fraction.

For the recovered particulate solids, define cobalt yield $Y_{\text{Co,s}}$ and cobalt mass fraction $w_{\text{Co,s}}$ on the same washed-solid basis. Their dry particulate mass is:

$$m_s = \frac{Y_{\text{Co,s}} m_{\text{Co,in}}}{w_{\text{Co,s}}} \quad (25)$$

Let $m_e = \rho_e V_e$ be retained solution mass, and s_e its nonvolatile dissolved-solids mass fraction. For drying which removes water while retaining uranium and nonvolatile salts:

$$m_{\text{product,wet}} = m_s + m_e, \qquad m_{\text{product,dry}} = m_s + s_e m_e \quad (26)$$

This distinction prevents dissolved salts left during drying from disappearing from the product denominator. The drying protocol must define moisture removal without unaccounted decomposition or material loss. Product uranium mass fractions follow:

$$w_{\text{U,wet}} = \frac{m_{\text{U,product}}}{m_{\text{product,wet}}}, \qquad w_{\text{U,dry}} = \frac{m_{\text{U,product}}}{m_{\text{product,dry}}} \quad (27)$$

Use consistent mass units. Multiplication by 10^6 converts a kg/kg mass fraction to mg/kg. This review defines the acceptance relation on a dry-product basis, with $w_{\text{U,lim,dry}}$ supplied by the applicable specification:

$$f_{\text{U,s}} m_{\text{U,in,Co}} + C_{\text{U,e}} V_e \le w_{\text{U,lim,dry}} (m_s + s_e m_e) \quad (28)$$

If the contractual specification uses wet product, replace the denominator by $m_s + m_e$ and use the corresponding wet-basis limit. No numerical acceptance limit is assumed here. These balances show why a liquor uranium target requires downstream transfer, cobalt yield, cake composition, and washing evidence. The symbols f, Y, w, and s_e are dimensionless fractions, not percentages. This derivation follows conservation of mass and does not represent new experimental data.

➢ *Thermodynamic Interpretation and its Limits*

The general Nernst relation and mineral saturation index are:

$$E_h = E^\circ - \frac{2.303RT}{nF} \log_{10} Q \quad (29)$$

ISSN No:-2456-2165 https://doi.org/10.38124/ijisrt/26aug1216

$$SI = \log_{10}\left(\frac{IAP}{K_{sp}}\right) \quad (30)$$

Here R is the gas constant, T absolute temperature, F the Faraday constant, n transferred electrons, and Q the dimensionless reaction quotient for the specified reduction reaction. Each redox couple has its own standard potential. The Nernst convention follows IUPAC (2025). The SI convention follows Parkhurst and Appelo (2013), with IAP and equilibrium constant defined for the same dissolution reaction.

Figure 1 relates aqueous speciation, solid formation, redox state, and rate processes to measured removal. Annex A supplies the reaction conventions needed to distinguish these contributions in a thermodynamic calculation.

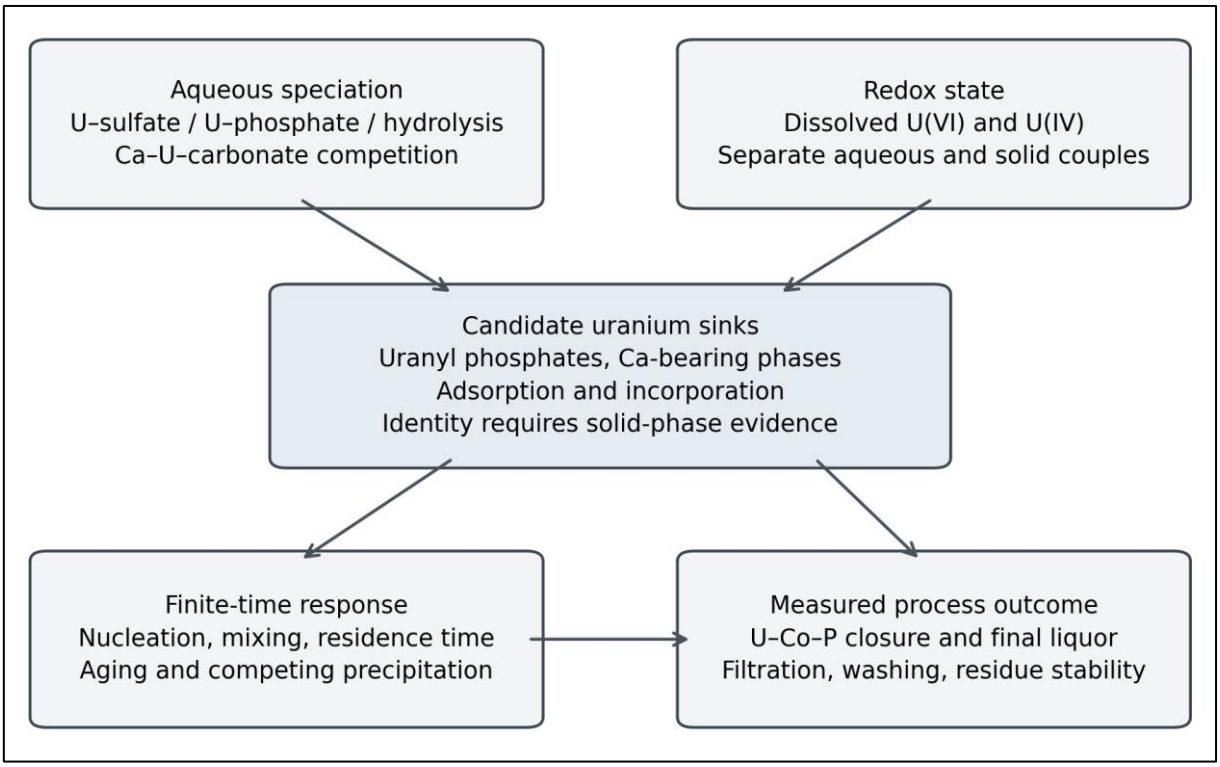

Fig 1 Conceptual Mechanism Framework Prepared for this Review. Connections Identify Coupled Processes. The Figure Provides no Numerical Stability Fields or Quantitative Performance Evidence.

A plant calculation requires measured analytical totals, temperature, a complete charge-balanced component set, an activity model, gas boundary conditions, and internally consistent aqueous and solid-phase data. Activity is generally calculated from composition and an adopted model rather than measured independently for every species. pH and redox measurements require stated electrode conventions and matrix-aware procedures. A bulk oxidation–reduction-potential reading need not equal the equilibrium potential of the uranium couple.

The suitability of an activity model depends on its parameter coverage. Pitzer and specific-ion-interaction formulations require interaction parameters covering the relevant uranium–phosphate–sulfate–cobalt system. Conditional constants measured in a supporting electrolyte require conversion before combination with infinite-dilution thermodynamic constants. The OECD Nuclear Energy Agency (2020) provides a reference basis for uranium thermodynamics.

Positive SI denotes thermodynamic supersaturation for the specified phase. It does not determine induction time, precipitate crystallinity, or attainable concentration at finite residence time. A metastable precipitate might govern short-term removal, while a different phase governs subsequent aging or dissolution. Thermodynamic interpretation and kinetic evidence therefore require separate reporting.

IV. COMPARATIVE EVIDENCE AND MECHANISTIC SYNTHESIS

➢ *Source Extraction*

Table 4 distinguishes operational reports, published design assumptions, and laboratory observations. Source locations refer to printed pages unless an abstract or institutional record is specified. Quantitative comparisons retain the authors' reporting bases.

ISSN No:-2456-2165 https://doi.org/10.38124/ijisrt/26aug1216

Table 3 Central-Study Index. Conditions, Outcomes, Uncertainty, and Source Locations are Separated in Supplement S1.

Study	Evidence basis	Role in this review
Van Deventer (2023)	A, operational account	Deployment and equipment reliability
Pretorius and Mautsa (2023)	A/B/D, consumption account and analytical tests	Residual-phosphorus measurement
Dempers et al. (2023)	D, conceptual design	Equipment and economic comparison
Mehta et al. (2014)	B, full text	Co-solutes and filtration cutoff
Mehta et al. (2016)	B, abstract-level pathway evidence	Addition-pathway effects
Gorman-Lewis et al. (2009)	B/C, full main text	Phase-specific solubility and thermodynamics
Pan et al. (2016)	B, full text	Sediment retention and release
Wellman et al. (2007)	B, full text	Acidic dissolution
Lammers et al. (2017)	B, field groundwater study	Flow, loading and phase evidence
Foster et al. (2019)	B, process-effluent experiments	Sulfate-rich matrix and separation
Szenknect et al. (2020)	B, synthetic/mining waters	Host dissolution and Cu release
Rao et al. (2026)	B, seeded synthetic solutions	Seed inventory and release
Gudavalli et al. (2013)	B, flow-through mineral dissolution	Bicarbonate-dependent residue release

➢ *Operational Evidence and Design Assumptions*

The Metalkol report supports phosphate treatment as an operational option under the circumstances described. Its feed concentration and treatment requirement belong to the process specification, rather than a paired removal test (Van Deventer, 2023). The account demonstrates the importance of equipment reliability alongside separation chemistry.

Pretorius and Mautsa (2023) report estimated demand of 2–3 t/d, supervised consumption of 4–6 t/d, and subsequent use exceeding 14 t/d at an unnamed facility. This account motivates dosage measurement. Their experiments establish colorimetric response in prepared solutions with Co/Cu additions, while the industrial feedback scheme remains proposed. Throughput and acid assay are not supplied for normalization of the consumption account. The relevant engineering inference is to validate residual-P measurement against independent uranium response and the actual liquor matrix.

Dempers et al. (2023) compare low initial expenditure for phosphate dosing with lower operating expenditure for IX under their design assumptions. Table 7 gives a USD 20.4 million capital difference, USD 7.55 million annual savings, and an 8% discount rate. These reproduce the 2.70-year simple payback. Discounted payback is 3.16 years under a fractional-period annuity convention or 3.17 years with linear interpolation within the fourth year. The reported 3.17 years is therefore compatible with a conventional calculation. The separate nine-year mine-life statement remains unexplained. A further inconsistency concerns acid consumption: applying the stated Fe(III)+U model, one P per Fe and per U, 20% excess, and 85% acid to Table 1 gives approximately 311 kg/h, at most 2726 t/year over 8760 h. Table 5 instead uses 5700 t/year. Supplement S1 provides the calculation. The reagent basis must be reconciled before the published paybacks support a site decision. Cobalt coprecipitation is discussed but not quantified.

These sources answer different questions. Operating experience establishes deployment, the analytical study tests a measurement response, and the design comparison examines an assumed equipment and cost basis. Agreement on the usefulness of phosphate treatment does not convert those different forms of evidence into a shared dose-response dataset.

Manzuk and Philippe (2026) add a regional carryover model and trade-record analysis. These contextual data motivate uranium accounting but do not measure the treatment response of an individual plant. Reagent imports are a proxy for use, not a measured assayed dose. Similarly, absence of an identified import record cannot establish absence of IX deployment, which Van Deventer (2023) reports at Metalkol. Regional model outputs therefore remain separate from the operational accounts and are not used to calibrate the product-transfer fraction in Section 4.6.

➢ *Why the Uranium-Retention Mechanism Changes*

Mehta et al. (2014, Table 1 and Sections 2.2–3.3) tested 100 µM uranium with nominal total phosphorus of 1 mM, at initial pH 4, 6, and 7.5 and 22 ± 0.5 °C, with observations through 10 days. Sodium, calcium, and DIC were varied separately. Cation-free systems formed chernikovite even where uranyl orthophosphate was thermodynamically preferred. Sodium shifted the products toward sodium autunite. With 5 mM calcium, autunite was detected at pH 4 and 6, whereas the pH 7.5 solid lacked its diffraction peaks and contained a poorly crystalline calcium-phosphate component. Calcium experiments at pH 4 and 6 gave residual uranium below 8.4×10^{-10} M after 10 days. The coupled calcium/phosphorus depletion and uranium concentrations below predicted autunite solubility support an additional calcium-phosphate-associated sink, but do not uniquely distinguish adsorption from incorporation.

The same study compared 0.22 and 0.05 µm filtration and tested filter sorption. Differences in filtrate uranium show that a separation cutoff can change the reported aqueous endpoint by retaining nanoparticles. A dose-response curve therefore requires a stated filtration protocol and a distinction between operationally filtered uranium and truly dissolved species. The nominal P/U ratio of ten describes reagent supply, not a measured mineral stoichiometry. Supplement S1 preserves the paper's 1.0 versus 1.1 mM phosphorus inconsistency in the calcium-series table and figure captions.

ISSN No:-2456-2165 https://doi.org/10.38124/ijisrt/26aug1216

The abstract of Mehta et al. (2016) reports that addition pathway changed uranium retention at pH 7.5. Simultaneous dissolved reactants favored incorporation into newly formed amorphous calcium phosphate, whereas preformed calcium phosphate favored adsorption. A suspension containing both preformed solids and dissolved calcium/phosphate produced mixed autunite precipitation and adsorption. At pH 4 and 6, autunite precipitation occurred across the tested starting forms. These qualitative assignments support addition-sequence controls. The abstract-reported mechanism fractions are retained in Supplement S1 with their unresolved uncertainty definition and are not used to set dose, residence time, or cobalt retention.

Pan et al. (2016) extend this distinction to sediment-bearing flow systems. Their columns used approximately 3.5 μM uranium during loading and 1 mM phosphate during treatment of loaded sediment. Phosphate treatment retained nearly six times more uranium than the comparison without phosphate, with enhanced retention persisting for at least one month after dosing ceased. Spectroscopy and extraction indicated predominantly adsorbed uranium in the columns. The result links phosphate addition to retention without requiring a discrete phosphate precipitate under every condition.

Table S4 in Supplement S1 connects each mechanism to observations, competing explanations, discriminating measurements, and dosing or cobalt-retention consequences. The comparative inference is a three-pathway framework. Discrete uranyl-phosphate precipitation requires a phase-consistent stoichiometric and saturation calculation. Adsorption requires the reactive surface inventory and its uptake response. Incorporation requires the formation and composition of a host precipitate. Calcium and FAM solids therefore affect both phosphorus consumption and the identity of the uranium sink. The same decrease in aqueous uranium has different dosing and residue implications under these pathways. Applied to the reviewed studies, the framework prevents three unsupported decisions: assigning a unique phosphate stoichiometry to an unresolved calcium-associated sink, transferring a mechanism partition into a cobalt-retention claim, and treating an equilibrium plateau time as an industrial precipitation residence time. These are source-based applications of the decision rules, rather than numerical operating recommendations.

- *Connecting Formation, Separation, and Release*

Gorman-Lewis et al. (2009) approached solubility from both saturation directions. Nonstoichiometric dissolution and decreased crystallinity complicate interpretation, and undetected secondary phases were not excluded. Agreement between reversal measurements supports the authors' equilibrium interpretation. It does not establish precipitation kinetics in cobalt liquor.

Wellman et al. (2007) show why low initial solubility and subsequent residue behavior require separate assessment. Meta-autunite dissolution responds strongly to pH over the investigated acidic range, with comparatively limited temperature sensitivity. Secondary phosphate formation also affects dissolved uranium release. These observations support testing washed treatment solids under the chemical conditions expected during storage and contact with process waters.

Gudavalli et al. (2013, Sections 2.1–2.3 and Table 1) provide a complementary alkaline-carbonate test. They exposed 0.25 g natural Ca-meta-autunite to 0.5–3 mM bicarbonate in 0.01 M TRIS buffer, at nominal pH 7–11 and 23–90 °C. Steady release was reached after approximately eight reactor-volume exchanges. The fitted bicarbonate-response exponent for Ca-autunite increased from 0.50 ± 0.12 at pH 7 to 1.09 ± 0.11 at pH 10. These are fitted response parameters, not removal fractions. The reported typical propagated rate uncertainty was approximately ±35% at 2σ. Greater post-reaction layer separation in the calcium material supports a structural contribution to release, while modeled secondary-phase saturation does not establish phase occurrence. The comparison motivates testing the actual washed residue against relevant DIC and pH, rather than assigning durability from the autunite name.

The framework links each proposed retention pathway to three complementary evidence streams: solution inventories, solid-phase evidence, and separation or release behavior. Environmental reactive-transport modelling (Wen et al., 2018) and phosphate biomineralization work (Morrison et al., 2021) provide additional context for transport and phosphorus supply. Their roles in this review remain mechanistic, rather than evidence of cobalt-circuit performance.

- *Matrix Composition, Host Dissolution, and Seed Inventory*

Foster et al. (2019, Table 1 and Section 4) provide a useful bridge between dilute-water chemistry and process-effluent treatment. Their spent-catalyst effluent contained 0.16 mM uranium, 0.24 M sulfate, and a reported ionic strength of 0.75 M at initial pH 0.86. Bench tests used 2 L, potassium dihydrogen phosphate, and pH 6.25. The reported conditions were 1 mM phosphorus for 30 min or 2 mM for 4 min at 25 °C, followed by filtration; uranium decontamination factors were at least 8000. The first dose corresponds to a total added P/U molar ratio of 6.25. XRD identified meta-ankoleite, and the bench separation included diatomite and a 0.1 μm polishing filter. Thus, both chemical treatment and the stated separation sequence contribute to the endpoint. Potassium-phosphate dosing and neutralization in this effluent cannot be converted directly into a phosphoric-acid requirement for a cobalt liquor.

Comparison at nominal total P = 1 mM illustrates why phosphate concentration alone is insufficient. Mehta et al. (2014) found a poorly crystalline calcium-phosphate component without detectable autunite peaks at pH 7.5 with 5 mM calcium, whereas Foster et al. (2019) identified meta-ankoleite in a sulfate-rich process effluent treated with potassium phosphate near pH 6.25. The studies differ in cation supply, pH, matrix, contact time, and separation. Their endpoints therefore support distinct host and process

ISSN No:-2456-2165 https://doi.org/10.38124/ijisrt/26aug1216

interpretations, not a common removal percentage or transferable acid dose.

Lammers et al. (2017, Tables 1–2 and Section 3) examined fish-bone-derived metastable hydroxyapatite in groundwater. Accelerated columns gave average uranium removals of 99.6% and 98.8% for two well waters, with mean influent concentrations of 2740 and 336 μg/L, respectively. These percentages are retained on their individual study bases. Chernikovite was identified in highly loaded column zones. Passive field canisters had unquantified water throughput, so their solid uptake does not establish a removal percentage. Local solid loadings exceeding 50 g U/kg also differ from whole-bed loading: the reported 21.8 g retained in column A1c corresponds to approximately 5.8 g/kg when divided by its 8.3 L bed volume and 0.45 kg/L bulk density. This calculated comparison shows why local phase evidence, total inventory, and flow must be connected before assigning a treatment capacity.

Szenknect et al. (2020, Tables 1, 2, and 4) compared copper-substituted hydroxyapatite in synthetic solutions and two mining waters. The mining-water tests used 0.3 g solid/L at room temperature, with uranium reaching a plateau after about four days. In acidic V105 water, the material with copper substitution parameter 1.59 reduced uranium from $(0.97 \pm 0.04) \times 10^{-6}$ to $(0.25 \pm 0.03) \times 10^{-7}$ M, while final aqueous copper was $(1.69 \pm 0.08) \times 10^{-4}$ M, approximately 10.7 mg/L. The quoted endpoint uncertainties describe variation among consecutive plateau samples. Diffraction identified meta-torbernite in the higher-uranium synthetic tests; phase assignments in the low-loading mining waters required more qualified interpretation. Host dissolution can therefore supply phosphorus and a uranium-binding cation while adding an impurity to the liquor. Uranium removal must be evaluated together with this reagent-derived metal transfer.

Rao et al. (2026, Sections 2.1–2.3) report 92% uranium depletion, from 50 to 4 μg/L, using 0.5 g/L meta-autunite seeds, added Ca:U:P = 50:1:10, pH 6, 25 °C, and 30 min. Their measured seed uranium content of 50.60 wt% implies approximately 253 mg U/L already present in seeds, about 5060 times the initial aqueous uranium inventory on the nominal dose basis. The reported aqueous depletion adds only about 0.018% of that seed uranium inventory. These calculations do not negate the measured filtrate response; they show that bulk identification of meta-autunite cannot by itself establish incremental precipitation of the trace feed uranium. A seed-only release control and an inventory-sensitive growth or tracer measurement are needed to distinguish uptake, seed dissolution, and recrystallization.

The Rao paper also lists model totals in Section 2.3 that differ by a factor of twenty from nominal concentrations calculated from the stated 50 mL recipe and from the uranium/phosphorus totals in Figure 5. The listed numbers correspond to reagent amounts in moles before division by volume. Supplement S1 records this inconsistency; its numerical speciation and predominance results are not adopted here. Together, these studies show that soluble phosphate dosing, dissolution of a phosphorus-bearing host, and treatment with uranium-bearing seeds have different initial inventories and different interpretations of an apparent removal percentage.

➢ *Evidence Limits and Transferability*

The central industrial sources establish operational experience, analytical feasibility, and conceptual process comparisons. They do not provide a complete measured dataset linking feed chemistry, assayed acid dose, time, temperature, uranium removal, cobalt retention, phase identity, separation, and residue release. The non-cobalt experimental studies resolve particular mechanisms without establishing joint uranium-removal/cobalt-retention performance in concentrated cobalt liquor. Source-specific access and uncertainty restrictions are recorded in Supplement S1 and limit the associated inferences. The targeted retrieval supports a structured critical review rather than exhaustive coverage. An unverified field is not evidence that the information is absent from the wider literature.

Transfer to concentrated cobalt sulfate liquors requires assessment of ionic strength, sulfate/carbonate complexation, competing cations, reactive solids, mixing, and contact time. This review supplies a chemical and accounting framework, not a calibrated plant model, a universal acid dose, or a validated residual-P setpoint. The two figures are conceptual. Quantitative uranium stability fields require specified composition, temperature, activity parameters, phase data, and reproducible calculations.

The resulting decision boundary is explicit. A treatment claim requires paired uranium and cobalt inventories with uncertainty. A mechanistic claim additionally requires uranium-host evidence. An operating recommendation further requires separation performance and independent validation in representative liquor. Product specifications, measured treatment endpoints, and final-product recovery remain separate quantities. These distinctions define the evidence required to progress from a plausible reaction to a justified process decision.

V. MINIMUM CALCULATION AND EXPERIMENTAL PROGRAMME

➢ *Representative Liquor and Analytical Controls*

Collect representative post-FAM liquor across the variability relevant to the intended application. Report source, collection date, storage, mixing before subsampling, elapsed time before testing, and dissolved versus particulate fractions. Measure U, Co, Cu, Fe, Al, Mn, Ca, Mg, Zn, sulfate, phosphorus, DIC, chloride, silica, suspended solids, pH, temperature, and density. Include other substantial ions detected by screening. Where oxidation state is relevant, use a validated speciation method rather than inferring U(VI)/U(IV) solely from bulk potential.

Specify the filter material and pore size used to define dissolved uranium. Test for sorption to filters and vessels. A filtered result is an operational fraction, and colloids below the cutoff require further separation if they influence the

ISSN No:-2456-2165 https://doi.org/10.38124/ijisrt/26aug1216

interpretation. Preserve paired total-element samples appropriately and measure pH and potential before preservation alters the sample.

Calibrate ICP-MS or another suitably sensitive method in the relevant matrix. Report dilution, internal standards, blanks, spikes, duplicates, calibration verification, LOQs, and uncertainty. Validate phosphorus measurement independently of uranium measurement. Distinguish elemental P, orthophosphate, and H_3PO_4-equivalent reporting. Analytical performance must support the applicable endpoint and the expected cobalt-loss difference.

When phosphate-bearing sorbents or uranium-bearing seeds are tested, include reagent-only release blanks and seed-free controls. Account for uranium initially present in solids, phosphorus released from the host, and introduced metals such as copper. Pair filtration-cutoff checks with filter-sorption blanks; report the operational definition of the aqueous fraction. Analytical repeats and consecutive kinetic samples do not replace independent reactor replication.

➢ *Staged Experiments and Independent Validation*

➢ *Thermodynamic Specification*

Convert measured laboratory concentrations into analytical molal totals using the measured solution composition, density, and water mass. Enter these calculated totals with the conversion basis and propagated uncertainty. Document software and database versions, modifications, standard states, reaction directions, log K values, temperature corrections, activity parameters, selected solids, and suppressed phases. Annex A defines the reaction conventions required for consistency. The calculation record is specified in Table A1.

Check electroneutrality and identify how any analytical imbalance is treated. Determine the importance of sulfate, carbonate, hydrolysis, and phosphate complexes before interpreting mineral saturation. Separate an equilibrium calculation with precipitation allowed from a speciation calculation constrained to the measured dissolved state. Report sensitivity to uncertain constants and phase selection. Validation requires parameter coverage appropriate to the measured ionic strength.

Table 4 Experimental Factors and Decision-Relevant Measurements. Numerical Levels Require Actual-Liquor Characterization.

Factor or control	Treatment basis	Required responses
Phosphorus addition	No-phosphate control, conditional stoichiometric basis, measured higher doses	U, Co, P in all phases
pH and neutralant	Bracket measured process range, record titration demand	Final pH, neutralant use, Co retention
Calcium, DIC, sulfate	Measured baseline and justified controlled variations	Speciation and phase sensitivity
Time and temperature	Relevant process conditions with kinetic sampling	Induction, rate, finite-time endpoint
Mixing and addition sequence	Record geometry, mixing conditions, dose location and duration	Reproducibility and precipitate properties
Suspended solids	Matched filtered and unfiltered liquor	Sorption, nucleation, entrainment
Replication	Initial independent triplicates at central and decision-critical conditions, followed by precision-based adjustment	Variance estimate, detectable difference, and confidence intervals
Independent liquor	Separate batch or campaign excluded from parameter fitting	Transferability of selected conditions

Begin with mechanistic tests in a chemically justified synthetic sulfate matrix, then assess actual liquor. A synthetic composition must derive from measured chemistry or a specified published dataset. Randomize run order and distinguish independent experimental replicates from repeat instrument readings. Include reagent blanks and neutralant-only controls. Record every sample withdrawal and replacement addition.

Use a staged design to avoid an impractically large full factorial. Establish the principal dose–pH–time response first, then examine composition and process interactions. Statistical analysis must match the design. Report effect sizes and confidence intervals, with model residuals where regression is used. Initial triplicates provide a starting estimate of experimental variability. Determine subsequent replication from this variability, the smallest cobalt-loss difference relevant to the decision, the chosen significance level, and statistical power. Distinguish independent batches from repeated aliquots or instrument readings.

Select the lowest tested dose meeting the joint uranium, cobalt-loss, phosphorus, and separation criteria with adequate uncertainty margin. Derive acceptance limits from the applicable product requirement and the downstream relationship between liquor uranium and product uranium.

Entering measured feed composition is model specification. Calibration applies only when selected parameters are adjusted against observations. State those parameters, bounds, and fitting targets. Validate against withheld experiments or an independent liquor batch. Compare predicted and measured dissolved uranium, phosphorus, cobalt transfer, and phase occurrence. If

ISSN No:-2456-2165 https://doi.org/10.38124/ijisrt/26aug1216

equilibrium is not reached, evaluate whether a kinetic model is necessary rather than fitting equilibrium constants to a transient endpoint.

➢ *Solids, Filtration, and Stability*

Measure recovered dry solid mass and U, Co, and P contents. Quantify entrained mother liquor and collect washing fractions. Use XRD and SEM-EDS as complementary first-line methods, with Raman, XANES, or EXAFS where necessary to resolve low-abundance or poorly crystalline uranium hosts. Failure to detect a phase by XRD does not establish its absence.

Measure settling behavior, filtrate clarity, filtration rate under stated pressure and geometry, cake moisture, and washing performance. Record aging time because phase transformation and aggregation alter separation. Characterize residue release under relevant acidic, alkaline, and carbonate-bearing exposures. Specify pH, DIC, temperature, liquid-to-solid ratio or flow-to-surface-area ratio, duration, and cumulative uranium release. A flow-through concentration plateau describes a steady release regime and does not by itself establish thermodynamic equilibrium or a residue service life. Section 6.4 links these requirements to the dissolution evidence.

➢ *Process Integration and Operational Interpretation*

Figure 2 places the treatment alternatives before cobalt recovery.

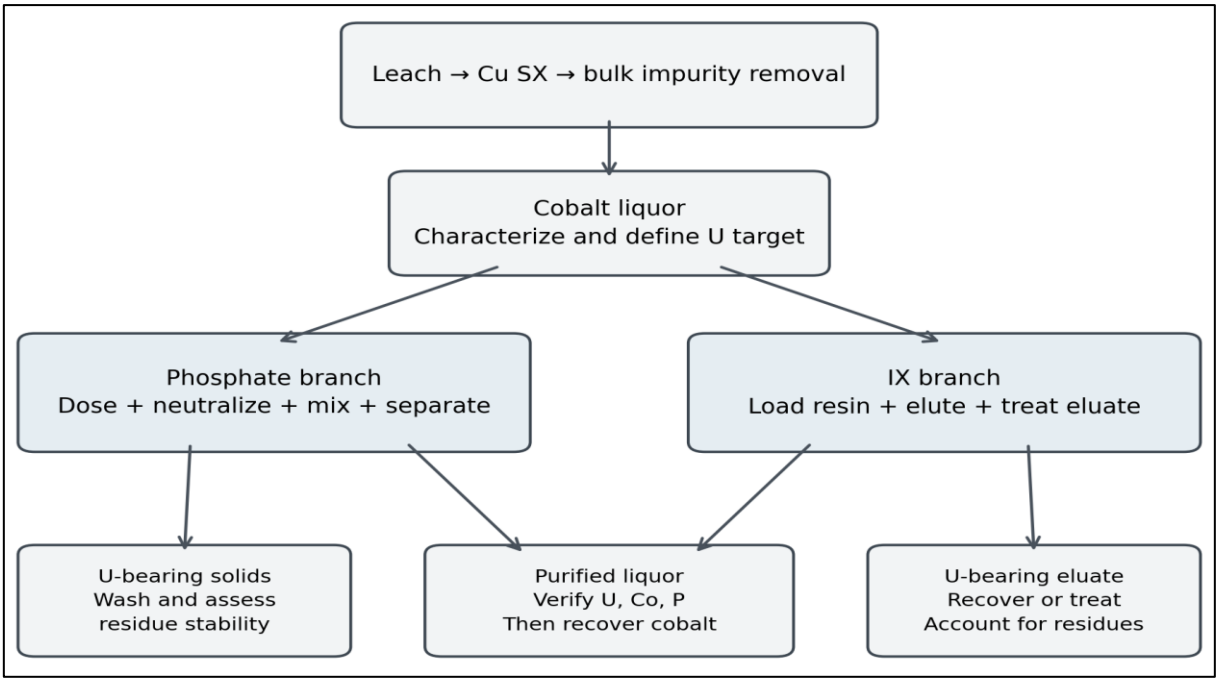

Fig 2 Conceptual Placement of Uranium Removal Before Cobalt Recovery. This Conceptual Flowsheet Identifies Alternative Branches and Accounting Streams. It Provides no Quantitative Performance Comparison.

Table 5 compares the corresponding engineering questions. Phosphoric acid introduces an additional solids-management duty, while IX transfers uranium to a resin and subsequently to an eluate. Neither route eliminates uranium accounting or residue treatment. A hybrid arrangement requires its own balance and operational justification.

Table 5 Qualitative Comparison for Site-Specific Option Assessment.

Criterion	Phosphate treatment	Ion exchange
Separation basis	Precipitation, adsorption, or incorporation	Loading of supported uranium species on a selected resin
Main chemical uncertainty	Competing P sinks and unidentified solids	Speciation, competing anions, capacity and elution
Cobalt accounting	Solid transfer, adsorption, entrainment	Co-loading, entrainment, losses in auxiliary streams
Main equipment questions	Dosing, neutralization, mixing, filtration	Contacting, hydraulics, resin transfer, elution
Uranium outlet	Separated precipitate and associated liquor	Eluate and subsequent recovery or treatment residues
Decision evidence	Actual-liquor dose response and filterability	Actual-liquor loading, breakthrough, elution and reliability
Economic basis	Reagent, neutralant, separation, Co loss, residue costs	Resin, chemicals, equipment, maintenance, eluate treatment

ISSN No:-2456-2165 https://doi.org/10.38124/ijisrt/26aug1216

Residual-phosphorus control requires matrix-validated measurement, sample conditioning, response-time characterization, and independent uranium confirmation. Detect instrument downtime, dilution error, and incomplete filtration. Feedforward demand estimation and feedback trimming then provide complementary responses to changing feed chemistry and measured residual phosphorus.

Assess commercial acid quality as a reagent input, including relevant metal impurities and uranium where material to the polishing balance. Treat neutralant consumption separately from acid dosage. Recirculated phosphorus and impurity buildup require a whole-circuit balance. A treatment performing well in an isolated batch might shift the burden to a downstream separation or recycle.

Uranium mass concentration in product, activity concentration of radionuclides, and external dose rate are different quantities. Record their respective units, analytical methods, and acceptance bases. Total uranium alone does not characterize all radionuclides in a residue or establish a universal radiation criterion. Any regulatory or shipment decision requires the current applicable specification and measurement protocol, which are outside the quantitative claims of this review.

VI. CONCLUSIONS

Phosphoric-acid uranium polishing combines several retention pathways whose relative importance depends on solution composition, phosphate supply, and the pre-existing solid inventory. The comparison of published evidence explains why equilibrium phase preference, observed precipitate identity, and dissolved uranium depletion require distinct interpretation. Calcium-bearing solids act both as phosphorus sinks and uranium hosts, while addition sequence changes the balance between precipitation, adsorption, and incorporation.

The contribution of this review is the connection of these mechanisms to an explicit measurement and decision framework. Phase stoichiometry establishes the conditional acid basis. Sampling-inclusive uranium and cobalt inventories establish transfer and selectivity. The downstream product balance connects residual liquor uranium to solid uptake, entrainment, cobalt yield, and dry- or wet-basis product specifications. Solid-phase characterization distinguishes the retention mechanism. Filtration, washing, and release tests establish whether the chemical response translates into a useful separation and a residue with characterized release under specified conditions.

Industrial accounts support phosphate treatment as an operating option and identify reagent consumption and equipment reliability as practical determinants. The next application of the framework is a representative-liquor programme connecting those determinants to measured U–Co–P balances. Such an integrated assessment provides the evidence needed to select dose, treatment placement, and control conditions within the transferability limits set out in Section 7.

ABBREVIATIONS

Table 6 Abbreviations Used in the Manuscript.

Abbreviation	Definition
DIC	Dissolved inorganic carbon
FAM	Iron–aluminium–manganese impurity removal
IAP	Ion activity product
ICP-MS / ICP-OES	Inductively coupled plasma mass / optical emission spectrometry
IX	Ion exchange
LOQ	Limit of quantification
NORM	Naturally occurring radioactive material
QA/QC	Quality assurance and quality control
SEM-EDS	Scanning electron microscopy with energy-dispersive X-ray spectroscopy
SHE	Standard hydrogen electrode
SI	Saturation index
SX	Solvent extraction
XANES / EXAFS	X-ray absorption near-edge / extended X-ray absorption fine structure
XRD	X-ray diffraction

REFERENCES

[1]. Avelar, É.C., C.L.G. Alvarenga, G.P.S. Resende, C.A. Morais, and M.B. Mansur, “Modeling of the Solvent Extraction Equilibrium of Uranium (VI) Sulfate with Alamine 336,” Brazilian Journal of Chemical Engineering, 34 (2017), 355–362. https://doi.org/10.1590/0104-6632.20170341s20150301.

[2]. Crundwell, F.K., N.B. du Preez, and B.D.H. Knights, “Production of Cobalt from Copper-Cobalt Ores on the African Copperbelt – An Overview,” Minerals Engineering, 156 (2020), 106450. https://doi.org/10.1016/j.mineng.2020.106450.

ISSN No:-2456-2165 https://doi.org/10.38124/ijisrt/26aug1216

[3]. Dempers, N.C.J., R.A. Wildenboer, and J.A.L. Parker, "Uranium Removal from Cobalt Process Liquor," Copper Cobalt Africa 2023 (Johannesburg: SAIMM, 2023), 177–188. https://www.saimm.co.za/Conferences/Copper-Cobalt-2023/19-Wildenboer-177-188.pdf.

[4]. Dong, W., and S.C. Brooks, "Determination of the Formation Constants of Ternary Complexes of Uranyl and Carbonate with Alkaline Earth Metals (Mg^{2+}, Ca^{2+}, Sr^{2+}, and Ba^{2+}) Using Anion Exchange Method," Environmental Science & Technology, 40 (2006), 4689–4695. https://doi.org/10.1021/es0606327.

[5]. Dzik, E.A., H.L. Lobeck, L. Zhang, and P.C. Burns, "Thermodynamic Characterization of Synthetic Autunite," American Mineralogist, 102 (2017), 1977–1980. https://doi.org/10.2138/am-2017-6109.

[6]. Foster, R.I., K.-W. Kim, M.-K. Oh, and K.-Y. Lee, "Effective Removal of Uranium via Phosphate Addition for the Treatment of Uranium Laden Process Effluents," Water Research, 158 (2019), 82–93. https://doi.org/10.1016/j.watres.2019.04.021.

[7]. Gorman-Lewis, D., T. Shvareva, K.-A. Kubatko, P.C. Burns, D.M. Wellman, B. McNamara, J.E.S. Szymanowski, A. Navrotsky, and J.B. Fein, "Thermodynamic Properties of Autunite, Uranyl Hydrogen Phosphate, and Uranyl Orthophosphate from Solubility and Calorimetric Measurements," Environmental Science & Technology, 43 (2009), 7416–7422. https://doi.org/10.1021/es9012933.

[8]. Gudavalli, R.K.P., Y.P. Katsenovich, D.M. Wellman, M. Idarraga, L.E. Lagos, and B. Tansel, "Comparison of the Kinetic Rate Law Parameters for the Dissolution of Natural and Synthetic Autunite in the Presence of Aqueous Bicarbonate Ions," Chemical Geology, 351 (2013), 299–309. https://doi.org/10.1016/j.chemgeo.2013.05.038.

[9]. Haynes, W.M., D.R. Lide, and T.J. Bruno, eds., CRC Handbook of Chemistry and Physics, 97th ed. (Boca Raton, FL: CRC Press, 2016). https://doi.org/10.1201/9781315380476.

[10]. International Union of Pure and Applied Chemistry (IUPAC), "Nernst Equation," Compendium of Chemical Terminology, 5th ed. (2025). https://doi.org/10.1351/goldbook.09068.

[11]. Lammers, L.N., H. Rasmussen, D. Adilman, J.L. deLemos, P. Zeeb, D.G. Larson, and A.N. Quicksall, "Groundwater Uranium Stabilization by a Metastable Hydroxyapatite," Applied Geochemistry, 84 (2017), 105–113. https://doi.org/10.1016/j.apgeochem.2017.06.001.

[12]. Manzuk, R.A., and S. Philippe, "Uranium in Cobalt-Hydroxide Exports from the Democratic Republic of the Congo," Nature Communications, 17 (2026), 7415. https://doi.org/10.1038/s41467-026-75910-z.

[13]. Mehta, V.S., F. Maillot, Z. Wang, J.G. Catalano, and D.E. Giammar, "Effect of Co-solutes on the Products and Solubility of Uranium(VI) Precipitated with Phosphate," Chemical Geology, 364 (2014), 66–75. https://doi.org/10.1016/j.chemgeo.2013.12.002.

[14]. Mehta, V.S., F. Maillot, Z. Wang, J.G. Catalano, and D.E. Giammar, "Effect of Reaction Pathway on the Extent and Mechanism of Uranium(VI) Immobilization with Calcium and Phosphate," Environmental Science & Technology, 50 (2016), 3128–3136. https://doi.org/10.1021/acs.est.5b06212.

[15]. Meija, J., T.B. Coplen, M. Berglund, W.A. Brand, P. De Bièvre, M. Gröning, N.E. Holden, J. Irrgeher, R.D. Loss, T. Walczyk, and T. Prohaska, "Atomic Weights of the Elements 2013 (IUPAC Technical Report)," Pure and Applied Chemistry, 88 (2016), 265–291. https://doi.org/10.1515/pac-2015-0305.

[16]. Morrison, K.D., M. Zavarin, A.B. Kersting, J.D. Begg, H.E. Mason, E. Balboni, and Y. Jiao, "Influence of Uranium Concentration and pH on U-Phosphate Biomineralization by Caulobacter OR37," Environmental Science & Technology, 55 (2021), 1626–1636. https://doi.org/10.1021/acs.est.0c05437.

[17]. OECD Nuclear Energy Agency, Second Update on the Chemical Thermodynamics of U, Np, Pu, Am and Tc, Chemical Thermodynamics, vol. 14, NEA No. 7500 (Paris: OECD Publishing, 2020). https://www.oecd-nea.org/upload/docs/application/pdf/2020-10/7500_second_update_of_u_np_pu_am_and_tc_web.pdf.

[18]. Pan, Z., D.E. Giammar, V. Mehta, L.D. Troyer, J.G. Catalano, and Z. Wang, "Phosphate-Induced Immobilization of Uranium in Hanford Sediments," Environmental Science & Technology, 50 (2016), 13486–13494. https://doi.org/10.1021/acs.est.6b02928.

[19]. Parkhurst, D.L., and C.A.J. Appelo, Description of Input and Examples for PHREEQC Version 3: A Computer Program for Speciation, Batch-Reaction, One-Dimensional Transport, and Inverse Geochemical Calculations, Techniques and Methods 6-A43 (Reston, VA: U.S. Geological Survey, 2013). https://doi.org/10.3133/tm6A43.

[20]. Pretorius, R., and N. Mautsa, "Online Measurement of Residual Phosphorus in the Cobalt Precipitation Process for the Purpose of Dosage Control," Copper Cobalt Africa 2023 (Johannesburg: SAIMM, 2023), 171–176. https://www.saimm.co.za/Conferences/Copper-Cobalt-2023/18-Pretorius-171-176.pdf.

[21]. Rao, J., P. Ke, T. Zhong, C. Wang, Y. Qin, Y. Zhou, L. Xu, J. Wang, G. Li, and Z. Sun, "Immobilization of Low-Concentration Uranium by Mineralization with Phosphates: Dissolution Stability of Meta-Autunite Products in the Presence of Coexisting Anions," Environmental Research, 307 (2026), 125457. https://doi.org/10.1016/j.envres.2026.125457.

[22]. Sole, K.C., J. Parker, P.M. Cole, and M.B. Mooiman, "Flowsheet Options for Cobalt Recovery in African Copper-Cobalt Hydrometallurgy Circuits," Mineral Processing and Extractive Metallurgy Review, 40 (2019), 194–206. https://doi.org/10.1080/08827508.2018.1514301.

ISSN No:-2456-2165 https://doi.org/10.38124/ijisrt/26aug1216

[23]. Szenknect, S., A. Mesbah, M. Descostes, A. Maihatchi-Ahamed, L. Bonato, M. Massonnet, Y. Ziouane, E. Vors, T. Vercouter, N. Clavier, J. Lautru, and N. Dacheux, "Uranium Removal from Mining Water Using Cu Substituted Hydroxyapatite," Journal of Hazardous Materials, 392 (2020), 122501. https://doi.org/10.1016/j.jhazmat.2020.122501.

[24]. Van Deventer, J., "Use of Ion Exchange to Increase Value in Copper-Cobalt Operations," Copper Cobalt Africa 2023 (Johannesburg: SAIMM, 2023), 321–332. https://www.saimm.co.za/Conferences/Copper-Cobalt-2023/32-van-Deventer-321-332.pdf.

[25]. Vercouter, T., P. Vitorge, B. Amekraz, and C. Moulin, "Stoichiometries and Thermodynamic Stabilities for Aqueous Sulfate Complexes of U(VI)," Inorganic Chemistry, 47 (2008), 2180–2189. https://doi.org/10.1021/ic701379q.

[26]. Vopálka, D., K. Štamberg, A. Motl, and B. Drtinová, "The Study of the Speciation of Uranyl-Sulphate Complexes by UV–Vis Absorption Spectra Decomposition," Journal of Radioanalytical and Nuclear Chemistry, 286 (2010), 681–686. https://doi.org/10.1007/s10967-010-0764-5.

[27]. Wellman, D.M., K.M. Gunderson, J.P. Icenhower, and S.W. Forrester, "Dissolution Kinetics of Synthetic and Natural Meta-Autunite Minerals, $X_{3-n}^{(n)+}[(UO_2)(PO_4)]_2 \cdot xH_2O$, under Acidic Conditions," Geochemistry, Geophysics, Geosystems, 8 (2007), Q11001. https://doi.org/10.1029/2007GC001695.

[28]. Wen, H., Z. Pan, D.E. Giammar, and L. Li, "Enhanced Uranium Immobilization by Phosphate Amendment under Variable Geochemical and Flow Conditions: Insights from Reactive Transport Modeling," Environmental Science & Technology, 52 (2018), 5841–5850. https://doi.org/10.1021/acs.est.7b05662.

ISSN No:-2456-2165 https://doi.org/10.38124/ijisrt/26aug1216

ANNEX

ANNEX A. BALANCED THERMODYNAMIC RELATIONS AND CONVENTIONS

➢ *A.1 Standard States and Phosphate Accounting*

For dissolved species, $a_i = \gamma_i b_i / b^\circ$, where $b^\circ = 1$ mol kg^{-1}. Gas fugacity ratios are dimensionless relative to their standard-state fugacity. Pure selected solids have unit activity. Water activity a_w refers to water in the solution and is not automatically unity in concentrated liquor. The following relations use conventional acid-dissociation constants, with the solvent convention applied consistently.

$$b_{\mathrm{P,T}} = b_{\mathrm{P,free}} + \sum_j \nu_{\mathrm{P},j}\, b_j \qquad (A1)$$

The sum covers phosphorus-bearing complexes excluded from the four free protonation forms, with $\nu_{\mathrm{P},j}$ phosphorus atoms per complex. For each protonation step, mass action gives, for example:

$$\frac{b_{\mathrm{H_2PO_4^-}}}{b_{\mathrm{H_3PO_4}}} = \frac{K_{a1}\gamma_{\mathrm{H_3PO_4}}}{a_{\mathrm{H^+}}\gamma_{\mathrm{H_2PO_4^-}}} \qquad (A2)$$

$$\frac{b_{\mathrm{HPO_4^{2-}}}}{b_{\mathrm{H_2PO_4^-}}} = \frac{K_{a2}\gamma_{\mathrm{H_2PO_4^-}}}{a_{\mathrm{H^+}}\gamma_{\mathrm{HPO_4^{2-}}}} \qquad (A3)$$

$$\frac{b_{\mathrm{PO_4^{3-}}}}{b_{\mathrm{HPO_4^{2-}}}} = \frac{K_{a3}\gamma_{\mathrm{HPO_4^{2-}}}}{a_{\mathrm{H^+}}\gamma_{\mathrm{PO_4^{3-}}}} \qquad (A4)$$

A total-phosphorus calculation must solve these relations together with complexation and component balances. The ideal fractions in Equation (8) result when the relevant activity-coefficient ratios approach one.

➢ *A.2 Water-Stability Reference Relations*

For oxygen reduction:

$$\mathrm{O_2(g) + 4H^+ + 4e^- \rightleftharpoons 2H_2O} \qquad (A5)$$

$$E_h = 1.229 - 0.05916\,\mathrm{pH} + 0.01479\log_{10}\left(\frac{f_{\mathrm{O_2}}}{f^\circ}\right) - 0.02958\log_{10} a_w \qquad (A6)$$

For hydrogen evolution:

$$\mathrm{2H^+ + 2e^- \rightleftharpoons H_2(g)} \qquad (A7)$$

$$E_h = -0.05916\,\mathrm{pH} - 0.02958\log_{10}\left(\frac{f_{\mathrm{H_2}}}{f^\circ}\right) \qquad (A8)$$

Equations (A6) and (A8) are expressed in volts versus SHE at 25 °C. With unit gas-fugacity ratios and unit water activity, they reduce to the conventional water lines. They are thermodynamic reference limits, not uranium-phase boundaries or gas-evolution rate predictions.

➢ *A.3 Uranyl Complexation and Hydrolysis*

The species list should include supported protonated uranyl-phosphate and hydrolysis reactions in addition to Equations (9)–(10):

$$\mathrm{UO_2^{2+} + H_2PO_4^- \rightleftharpoons UO_2H_2PO_4^+} \qquad (A9)$$

$$\mathrm{UO_2^{2+} + H_2O \rightleftharpoons UO_2OH^+ + H^+} \qquad (A10)$$

$$\mathrm{2UO_2^{2+} + 2H_2O \rightleftharpoons (UO_2)_2(OH)_2^{2+} + 2H^+} \qquad (A11)$$

ISSN No:-2456-2165 https://doi.org/10.38124/ijisrt/26aug1216

Additional species follow the selected database, composition, and model scope.

➢ *A.4 Phosphate Solids and Matching Dissolution Constants*

Hydronium uranyl phosphate trihydrate, $H_3O(UO_2)(PO_4)\cdot 3H_2O$, is compositionally equivalent to $UO_2HPO_4\cdot 4H_2O$. Gorman-Lewis et al. (2009, Table 2) instead report HUP as $UO_2HPO_4\cdot 3H_2O$. Keep these hydrate definitions separate. For the four-water bookkeeping formula:

$$UO_2HPO_4 \cdot 4H_2O(s) \rightleftharpoons UO_2^{2+} + HPO_4^{2-} + 4H_2O \qquad (A12)$$

$$K_{HUP,4} = a_{UO_2^{2+}} a_{HPO_4^{2-}} a_w^4 \qquad (A13)$$

For uranyl orthophosphate tetrahydrate:

$$(UO_2)_3(PO_4)_2 \cdot 4H_2O(s) \rightleftharpoons 3UO_2^{2+} + 2PO_4^{3-} + 4H_2O \qquad (A14)$$

$$K_{UP} = a_{UO_2^{2+}}^3 a_{PO_4^{3-}}^2 a_w^4 \qquad (A15)$$

For a specified calcium uranyl phosphate hydrate:

$$Ca(UO_2)_2(PO_4)_2 \cdot nH_2O(s) \rightleftharpoons Ca^{2+} + 2UO_2^{2+} + 2PO_4^{3-} + nH_2O \qquad (A16)$$

$$K_{CaUP,n} = a_{Ca^{2+}} a_{UO_2^{2+}}^2 a_{PO_4^{3-}}^2 a_w^n \qquad (A17)$$

Each equilibrium constant applies to a fixed hydrate number n. Equilibrium constants published for $H^+ + PO_4^{3-}$ dissolution components require transformation before use with an HPO_4^{2-} activity product. The relevant acid-dissociation constant supplies that transformation. Likewise, a database convention omitting explicit solvent activity must not be combined with a different reaction quotient without justification. Gorman-Lewis et al. (2009) and OECD Nuclear Energy Agency (2020) are starting sources for the necessary phase and reaction data.

➢ *A.5 Distinct U(VI)/U(IV) Reduction Couples*

Dissolved uranyl reduction to dissolved U^{4+} is:

$$UO_2^{2+} + 4H^+ + 2e^- \rightleftharpoons U^{4+} + 2H_2O \qquad (A18)$$

At 25 °C:

$$E_h = E_1^\circ - 0.11832\,\mathrm{pH} - 0.02958\log_{10}\left(\frac{a_{U^{4+}}}{a_{UO_2^{2+}}}\right) - 0.05916\log_{10} a_w \qquad (A19)$$

At fixed dissolved-species activity ratio and water activity, its slope is −0.11832 V per pH unit. The solid UO_2 couple is instead:

$$UO_2^{2+} + 2e^- \rightleftharpoons UO_2(s) \qquad (A20)$$

$$E_h = E_2^\circ + 0.02958\log_{10} a_{UO_2^{2+}} \qquad (A21)$$

Here E_1° and E_2° refer to different reactions and are not interchangeable. Equation (A20) contains neither H^+ nor water. Consequently, Equation (A21) has no explicit pH term at fixed free uranyl activity and unit solid activity. A total-uranium boundary is conditional because pH-dependent complexation changes free uranyl activity. Its shape must be calculated for the specified total composition and supported phases.

Dissolved U(IV) hydrolysis introduces further species:

$$U^{4+} + H_2O \rightleftharpoons UOH^{3+} + H^+ \qquad (A22)$$

$$UOH^{3+} + H_2O \rightleftharpoons U(OH)_2^{2+} + H^+ \qquad (A23)$$

Uranium oxidation-state measurements and redox-equilibrium assessment determine which of these species belong in the liquor model.

ISSN No:-2456-2165 https://doi.org/10.38124/ijisrt/26aug1216

➢ *A.6 Numerical Model Documentation*

Table A1 Thermodynamic Specification Record for a Reproducible Calculation.

Data family	**Required record**
Analytical totals	Complete composition, water mass, charge balance, and uncertainty
Aqueous constants	Balanced reaction, log K, source, temperature, and standard state
Solid phases	Exact formula, hydrate, crystallinity, and dissolution convention
Activity model	Formulation, interaction-parameter coverage, and sensitivity
Redox	Couple-specific potentials and imposed or calculated state
Gas and solvent	Fugacity conditions and water-activity convention
Validation	Independent solution and phase observations, residuals, and uncertainty

ISSN No:-2456-2165 https://doi.org/10.38124/ijisrt/26aug1216

ANNEX B. COMPLETE BALANCE AND UNCERTAINTY REPORTING

For element i over a finite test interval, the general closure is:

$$\varepsilon_i = \frac{I_{i,f} + \sum m_{i,\text{out}} - I_{i,0} - \sum m_{i,\text{in}}}{I_{i,0} + \sum m_{i,\text{in}}} 100\% \qquad (B1)$$

$I_{i,0}$ and $I_{i,f}$ are the initial and final inventories within the boundary. Inputs include reagent impurities and replacement liquids. Outputs include samples, withdrawn products, washes leaving the boundary, and collected residues. A residue counted as final inventory is not counted again as an output. Positive closure error indicates excess accounted output plus final inventory relative to input plus initial inventory.

For continuous operation, integrate the time-dependent stream flows over the same interval. At steady state, inventory accumulation vanishes only after operational stability has been established. Report uranium, cobalt, and phosphorus closure separately. Report the residual difference explicitly rather than assigning it to an unidentified phase.

Uncertainty includes concentration, volume or flow, solid mass, moisture correction, and sampling representativeness. Shared calibration and dilution errors introduce covariance. For a derived response $y = f(\mathbf{x})$, a first-order estimate is:

$$u^2(y) \simeq \nabla f^{\mathsf{T}} \, \Sigma \, \nabla f \qquad (B2)$$

Here Σ is the input covariance matrix. Use an alternative uncertainty method when nonlinearity, censoring, or proximity to zero makes linear propagation inappropriate. A mass-balance acceptance interval follows from measurement uncertainty and the intended decision.